Ruggedizing Cryogenically Cooled Infrared Detectors

A.Veprik[1], N.Ashush[1], B. Shlomovich[1],Y. Oppenhaim[1], Y. Gridish[1], E. Kahanov[1], A. Koifman[1], A.Tuito[2]

[1]SemiConductor Devices (SCD), POB 2250, Haifa 31021, Israel
[2]Israel Ministry of Defense, Kirya, Tel Aviv, 64734, Israel

ABSTRACT

Cryogenically cooled infrared electro-optical payloads have to operate and survive frequent exposure to harsh vibrational and shock conditions, typical of the modern battlefield. This necessitates the ruggedizing of their sensitive components, such as the Integrated Dewar-Detector Assemblies (IDDA), the infrared Focal Plane Arrays (FPA) which are usually supported by a thin-walled cold finger enveloped by an evacuated tubular dewar. Without sufficient ruggedization, the harsh environmental vibration may give rise to structural resonances affecting image quality and reliability due to material fatigue.

The authors present their approach for the ruggedization of the IDDA by supporting the FPA using a mechanical support member extending from the dynamically damped dewar envelope. A mathematical model relies on an experimentally evaluated set of frequency response functions. By adding only 2% to the weight of the IDDA, the authors have managed to attenuate by 3-fold the relative deflection and absolute acceleration of the FPA.

INTRODUCTION

Integrated Dewar-Detector Assemblies (IDDAs) of cryogenically cooled infrared electro-optical payloads are known to be extremely susceptible to the vibration extremes, typical of the modern battlefield. Ruggedizing their critical components is therefore imperative, ensuring long-term endurance and stable optical performance.

Figure 1 shows a schematic depiction of a typical IDDA, where the cold finger is formed by a cold finger base and a tubular thin walled member extending from the base and sealed with the plug on its distal end. An infrared focal plane array (FPA) is attached, both mechanically and thermally, to the cold finger plug.

In order to reduce both the conductive and convective portions of the parasitic heat load, the thin-walled cold finger tube is made from a material with a low thermal conductivity (stainless steel or Titanium) and is enveloped by evacuated dewar extending from the cold finger base. The FPA is mounted behind an infrared transparent window, positioned at the distal end of the dewar envelope.

In this arrangement, the cold finger supporting the infrared detector is a slender, lightly damped, tip-mass cantilever typically responding to the environmental disturbance by developing

Cryocoolers 18, edited by S.D. Miller and R.G. Ross, Jr.

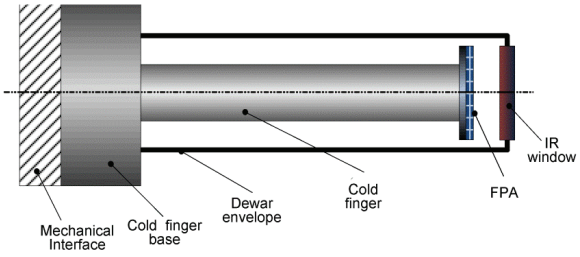

Figure 1. Schematic diagram of the IDDA

a large dynamic response, the magnitude of which can be comparable to the pixel size and thus degrade the image quality.

Attempts at stiffening the cold finger by increasing its thickness or by adding some stiffening features at its warm (proximal) end have been reported previously [1]. Attempts have also been reported on supporting its cold (distal) end by implementing a mechanical support member extending from the evacuated dewar envelope [2,3,4]. In one implementation the support member takes the form of a truncated conical metal tube with a low thermal conductivity [2] connected to the dewar base at its proximal (warm) end and to the distal (cold) end of the cold finger. In the second implementation [3], the support member takes the form of a composite low heat conductive star-wise disk, the central bore of which is fitted tightly around the cold finger distal (cold) end while its circumstantial portion is fitted tightly inside the bore at the distal end of the evacuated dewar. In the third implementation [4], an annular supporting structure is made of Titanium and comprises an upper and lower coaxial rings with reinforced ribs connecting said supporting rings. The upper ring is attached to the dewar base and a lower ring is tightly clamped around the cold finger tube using a suitable epoxy resin.

SCD has recently developed a technology of dewar ruggedizing, based on using supporting strings connecting the distal end of the rugged dewar envelope and cold finger tip. The strings are made of a material with a high stiffness and a low thermal conductivity [5].

The evident penalties of this approach are an increase in the conductive parasitic heat load resulting in elevated power consumption and heat rejection, lower life expectancy and higher vibration export produced by the mechanical (Stirling, typically) cryogenic cooler.

The efficiency of such an approach appears to be quite limited, especially in cases where the vibrational profile contains enough energy over the entire frequency range. Although the resonant frequency of the dewar envelope usually falls well above the typical 2 kHz margin, a dynamic coupling with the FPA mounted on the cold finger tip results in a combined dynamic system showing a very sharp resonant amplification occurring well below the 2 kHz margin. Typical is a 2-fold increase in the first resonant frequency (from, say, 800Hz to 1600Hz) and a 4-fold decrease in the damping ratio (from, say, 2% to 0.5%). In the case of "high frequency" vibration profiles typical of airborne applications, supporting the cold finger tip may be useless for controlling the FPA deflection; the penalties involve extra heat loading due to parasitic conduction, and higher levels of acceleration experienced by the FPA.

Simultaneous reduction of the relative deflection and absolute acceleration of said FPA will be possible in the case of a very rigid dewar envelope and a support member shifting the typical resonant frequencies well above the 2 kHz margin. Stiffening the dewar envelope, however, is not always feasible because of the added bulk to the electro-optical package. Along these lines, further stiffening of the front support member leads to an elevated heat load and is not feasible in the majority of cases. Improper design of the dewar envelope and support member can make the situation even worse.

Essential damping effect may be produced by using the concept of a wideband dynamic absorber. In [6], the authors succeeded to mitigate the problem of cooler induced microphonics by attaching such a device to a rear cover of the cold head of a split Stirling cryogenic cooler integrated with the slip-on dewar. Because of the strong dynamic coupling between external and

internal parts of IDDA, the typical high frequency resonant amplifications occurring at the FPA location were attenuated ten-fold, the rms responses were attenuated three-fold.

The authors are expanding the concept of wideband dynamic damping for the case of environment induced vibration. They capitalize on the fact that the front support of the distal end of the cold finger using support member extending from the dewar envelope introduces a very strong dynamic coupling between these dynamic sub-systems. Applying a wideband dynamic absorber externally to the dewar envelope (patent pending) will therefore be able to attenuate the dynamic response of the cold finger and, therefore, the FPA.

The authors make use of a newly developed approach to mathematical modeling and optimal design of a wideband dynamic absorber [6,7]. In this approach, the detailed knowledge of the mechanical properties/models of sub-systems or their finite element models is not needed at all. Instead, they use the set of complex frequency response functions (FRF) captured on an actual reference system (comprised of the cold finger carrying the FPA, dewar envelope and front support member) under the operational vibration profile. The wideband dynamic absorber is modeled as a lumped, damped sprung mass, the complex FRF of which is expressed through its mass, resonant frequency and damping ratio. A special technique is then applied to combine the said complex FRFs and thus to obtain the new set characterizing the combined system. The resulting set of new complex FRFs, therefore, relies on those of the reference system (with no dynamic absorber) and the parameters of the lumped dynamic absorber. This allows calculation of the dynamic response of the cold finger and performing parametric numerical optimization. Using the technique explained above, the authors have managed to attenuate the rms deflection of the FPA by a factor of 3 using a lightweight, 25 gm, dynamic absorber (adding approximately 2% to the weight of the entire IDDA) under realistic environmental conditions typical of airborne MWS (missile warning system) applications. The theoretical predictions are in fair agreement with the results of full-scale testing.

EXPERIMENTAL TESTING OF A STATE OF THE ART IDDA

Figure 2 shows the schematics of a state of the art Detector-Dewar portion of a typical IDDA, which is similar to that in Figure 1, with the exception of a mechanical support member (shown schematically as a flat disc) at the front which is placed between the distal (cold) end of the cold finger and the distal end of dewar envelope.

In Figure 2, $X_0(j\omega) = \int_{-\infty}^{\infty} x_0(t)\, e^{-j\omega t} dt$ is the complex Fourier transform of the absolute base vibrational motion given by the time function $x_0(t)$, where ω is the angular frequency and $j = \sqrt{-1}$ is the complex unity. Similarly, $X_{1,2}(j\omega) = \int_{-\infty}^{\infty} x_{1,2}(t)\, e^{-j\omega t} dt$ are the complex Fourier transforms of the cold finger tip and dewar envelope vibrational motion, respectively.

The appropriate power spectral densities (PSD) of displacements and accelerations will be further denoted as $X_0(\omega), X_1(\omega), X_2(\omega)$ and $A_0(\omega), A_1(\omega), A_2(\omega)$, respectively.

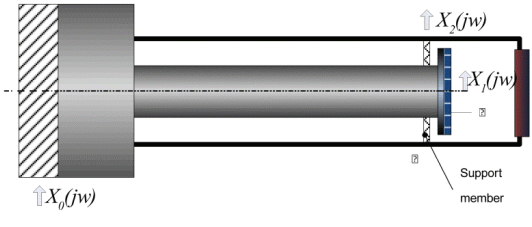

Figure 2. Schematic of the IDDA with front support

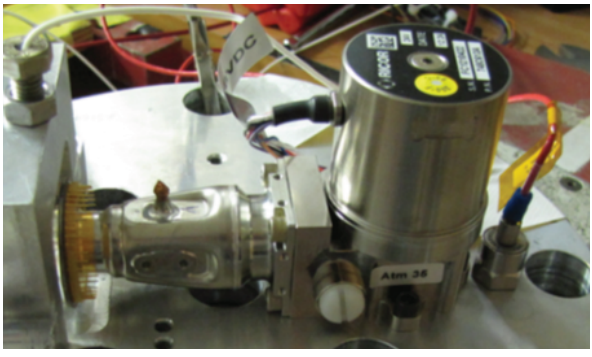

Figure 3. IDDA undergoing vibration testing

Figure 3 shows the actual IDDA under vibration test. Miniature accelerometers are mounted in locations ① and ② and monitor the absolute accelerations of the FPA and dewar envelope, respectively. In all further testing, the vibration profile per MIL-STD 810F will be characterized by the uniform power spectral density $A_0(\omega)=0.013g^2/Hz$ over the frequency range 10-2000Hz, totaling 5 g rms.

For the first test, the front support member was removed and the dynamic responses were studied of the unsupported FPA, and of the dewar envelope. The results are summarized in Figure 4. In particular, Figure 4.a shows the superimposed acceleration PSDs of the base, $A_0(\omega)$, the cold finger tip $A_1(\omega)$ and the dewar envelope, $A_2(\omega)$, respectively. In Figure 4.a, the dynamic response of the cold finger shows a well pronounced resonance at approximately 800Hz, while the resonance of the dewar envelope is well above the 2kHz margin. Figure 4.b shows the superimposed moduli of absolute transmissibility for the FPA and the dewar envelope. In Figure 4.b they are denoted as the reference transmissibilities, $|T1,2\,\mathrm{ref}|$. The frequency range in Figure 4.b is extended to 3kHz, in order to demonstrate that the dewar envelope resonance occurs at approximately 2100Hz. In Figure 4.b the resonant amplification of the dewar envelope is much higher, namely 165, as compared with 25 of the cold finger. Figure 4.c shows superimposed PSD curves of relative deflection for the FPA and for the dewar envelope, evaluated indirectly using the complex form of the absolute transmissibility,

$$X_1(\omega)=\left|T_1(j\omega)-1\right|^2 A(\omega)\omega^{-4} \tag{1}$$

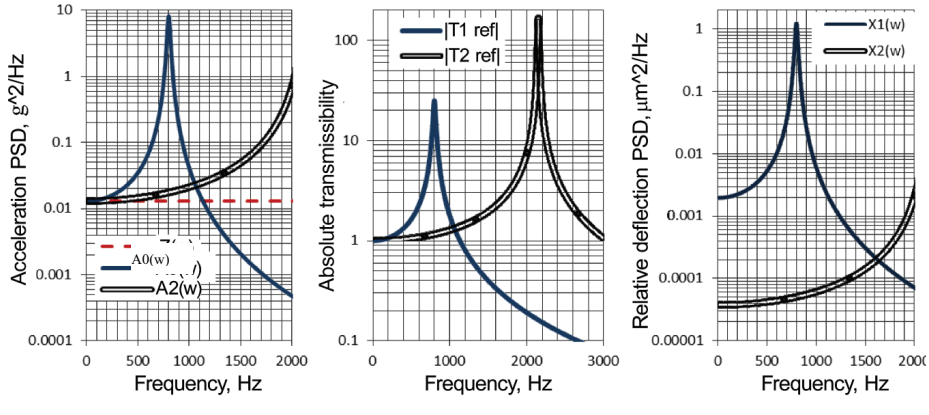

(a) (b) (c)

Figure 4. Dynamic responses of the FPA and dewar envelope

From Figures 4.a,b, the cold finger with FPA and dewar envelope behave very similarly to lightly damped single degree of freedom (SDOF) systems. From SDOF curve-fitting, the modal frequencies and damping ratios are 800Hz and 2% for the cold finger and 2150Hz and 0.3% for the dewar envelope, respectively. From the experimental test results, the overall (rms) acceleration and relative deflection levels are 20 g rms and 7.8 µm rms for the cold finger tip and 11 g rms and 0.6 µm rms for the dewar envelope, respectively.

In the second test, the front support member was mounted and the dynamic responses of the FPA and dewar envelope were studied. The results are summarized in Figure 5. In particular, Figure 5.a shows superimposed acceleration PSDs, $A_0(\omega)$, $A_1(\omega)$ and $A_2(\omega)$. Figure 5.b shows the superimposed moduli of absolute transmissibility for the cold finger tip and for the dewar envelope.

Figure 5.c shows superimposed PSDs of relative deflection for the FPA and for the dewar envelope, evaluated indirectly using the complex form of the absolute transmissibility, based on formula (1).

From Figures 5.a,b,c, the combined system "cold finger with FPA + front support member + dewar envelope" behaves as a lightly damped 2DOF dynamic system. The first observed resonant frequency is essentially higher than that of the unsupported FPA, because of the added stiffness; the penalty, however, is the higher amplification at resonance.

The explanation is trivial: adding stiffness without affecting damping results in a reduction of the effective damping ratio, which manifests itself in the form of elevated resonant amplification.

The overall acceleration and relative deflection of the FPA are 84 g rms and 7 µm rms, respectively.

Comparing the outcomes of the first and second tests, we can conclude that the resonant frequency of the combined system is still within the range of the vibration profile and that the resonant amplification is extremely high, because there is insufficient stiffness and a lack of damping in the dewar envelope and support member. The combination of these unfavorable factors results in only a minor attenuation of 12% in the relative deflection of the FPA, and a massive 4-fold amplification of the acceleration response. An additional penalty was a 40mW increase in the dewar heat load at 77K@23C.

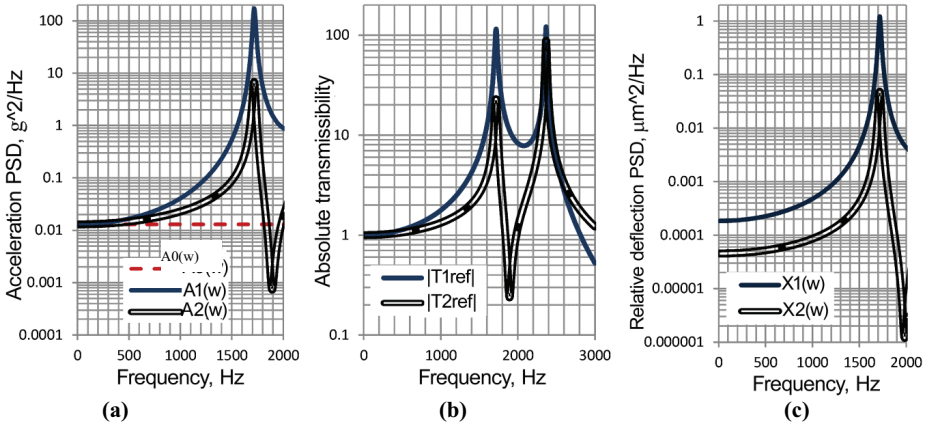

Figure 5. Dynamic responses of the combined system

DYNAMIC RUGGEDIZATION OF IDDA USING WIDEBAND DYNAMIC ABSORBER – THEORETICAL BACKGROUND

Figure 6 shows the schematics of a dynamically ruggedized IDDA (a) with a wideband dynamic absorber (b), mounted externally on the dewar envelope adjacent to the location of the support member. In one of the possible embodiments, the wideband dynamic absorber is made for compactness, from a composite (Silicone) bush carrying an inertial ring made from Tungsten. The central portion of the said bush is squeezed between two flat washers using a nut and a threaded stud, the free end of which is attached to the dewar envelope using a mounting stud.

The mathematical model of the combined system in the frequency domain will rely on the technique of complex frequency response functions and the superposition principle, see [6,7]. The absolute displacements of the "modified" system in the chosen locations ① and ② are again thought of as a superposition of the base induced motion and the response to the stimulus produced by the motion of dynamic absorber relative to its point of its attachment: $(K+j\omega B)\left[X_2(j\omega)-X_3(j\omega)\right]$. This can be written in the form

$$\begin{aligned} X_1(j\omega) &= T_1(j\omega)X_0(j\omega) - H_{21}(j\omega)(K+j\omega B)\left[X_2(j\omega)-X_3(j\omega)\right] \\ X_2(j\omega) &= T_2(j\omega)X_0(j\omega) - H_{22}(j\omega)(K+j\omega B)\left[X_2(j\omega)-X_3(j\omega)\right] \\ X_3(j\omega) &= T(j\omega)X_2(j\omega) \end{aligned} \tag{2}$$

In equations (2), $T_{1,2}(j\omega)$ are the absolute complex transmissibilities of the FPA and dewar envelope, $H_{22}(j\omega)$ and $H_{12}(j\omega)$ are the local and transitional complex receptances of the dewar envelope, $T(j\omega)=(K+j\omega B)\big/\left(-M\omega^2+K+j\omega B\right)$ is the single-mode approximation of the complex absolute transmissibility of the lumped wideband dynamic absorber expressed in terms of its mass M, spring constant K and damping factor B. The solution to equations (2) is trivial and produces a set of two complex transmisibilities for the combined system

$$\begin{aligned} \mathbf{T}_2(j\omega) &= \frac{X_2(j\omega)}{X_0(j\omega)} = \frac{T_2(j\omega)}{1-M\omega^2 H_{22}(j\omega)T(j\omega)} \\ \mathbf{T}_1(j\omega) &= \frac{X_1(j\omega)}{X_0(j\omega)} = T_1(j\omega) + M\omega^2 H_{21}(j\omega)T(j\omega)H_{22}(j\omega) \end{aligned} \tag{3}$$

Calculation of the power spectral densities and the root mean square (rms) values of the FPA relative deflection and acceleration in the combined system when subjected to a vibration profile given by the acceleration PSD, $A_0(\omega)$, is trivial:

$$\ddot{X}_1(\omega) = \left|\mathbf{T}_1(j\omega)\right|^2 A_0(\omega);\ X_1(\omega) = \left|\mathbf{T}_1(j\omega)-1\right|^2 A_0(\omega)\omega^{-4}; \tag{4,5}$$

$$\sigma_A = \sqrt{\frac{1}{2\pi}\int_0^\infty \ddot{X}_1(\omega)\,d\omega};\ \ \sigma_X = \sqrt{\frac{1}{2\pi}\int_0^\infty X_1(\omega)\,d\omega} \tag{6,7}$$

From equations (3), the dynamic properties of the combined system depend on those of the reference system and the properties of the dynamic absorber: M, K and B. They may be modified so as to minimize the rms displacement of FPA, σ_X. The optimization procedure with $M = 0.025kg$ yields the optimum resonant frequency $\Omega/2\pi = 1/2\pi\sqrt{K/M} = 1600Hz$ and damping ratio $\zeta = B/2M\Omega = 0.15$.

Figure 7 portrays the absolute transmissibilities of the FPA before and after mounting the optimized dynamic absorber upon the dewar envelope, from which follows that the dynamic absorber yields massive suppression of the resonant phenomena over the entire frequency range. This results in massive attenuation of the acceleration and relative deflections, as shown in Figures 8.a,b comparing PSD of the acceleration and relative deflection before and after the mounting of the dynamic absorber. The overall rms acceleration and deflection responses of the FPA are almost 3-fold attenuated from 86 g rms to 26 g rms and from 7.3 μm rms to 2.4 μm rms.

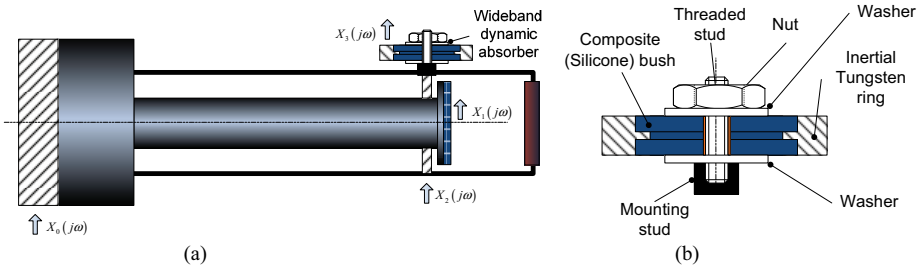

Figure 6. Schematics of wideband dynamic absorber.

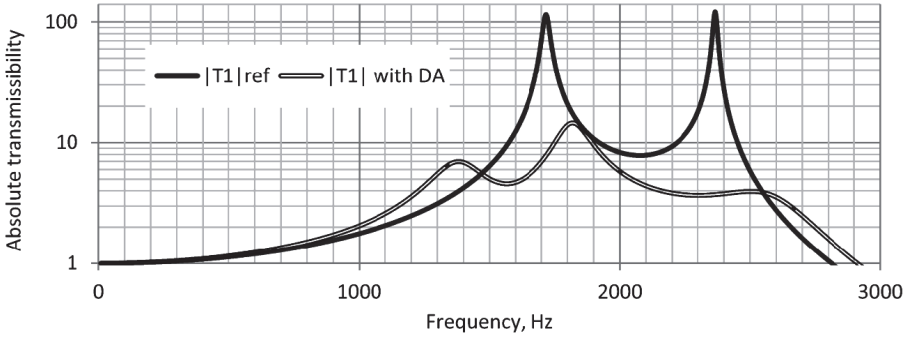

Figure 7. Modified dynamic responses of FPA

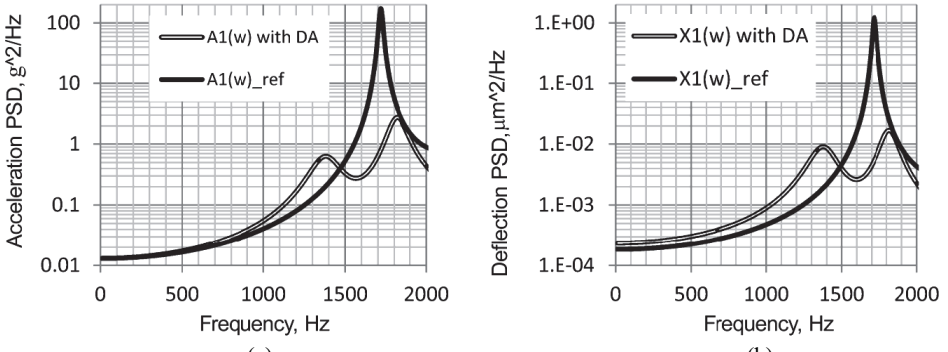

Figure 8. Modified dynamic responses of FPA

For the sensitivity analysis we will keep the optimal value of the resonant frequency (1600Hz) and vary the damping ratio of the dynamic absorber. Then we will keep the optimal value of the damping (15%) and vary the resonant frequency of the dynamic absorber. Figure 9 shows the sensitivity curves, from which the absorber parameters may depart somewhat from their optimal values practically without affecting the attainable performance.

FEASIBILITY STUDY AND ATTAINED PERFORMANCE

Figure 10 shows the experimental setup, where the wideband dynamic absorber is mounted upon the dewar envelope as explained above in Figure 6. Fine tuning has been performed by means of squeezing the elastomeric member (COTS EAR Isodamp grommet) between two flat washers. The material of the grommet is known to be capable of maintaining consistent mechanical properties over a wide temperature range and lifetime.

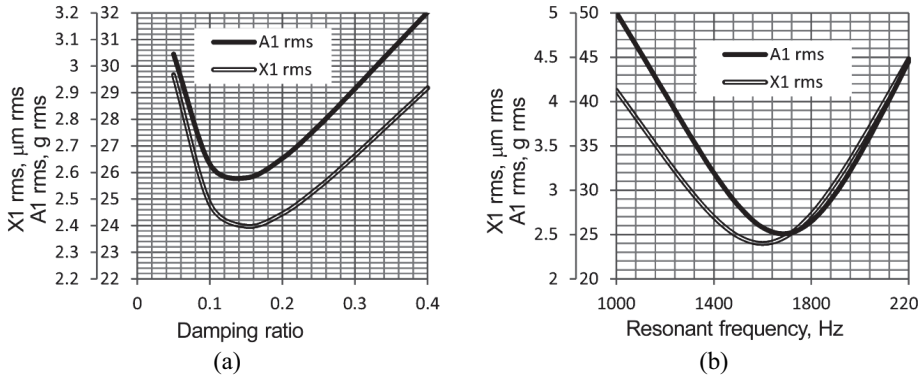

Figure 9. Sensitivity analysis

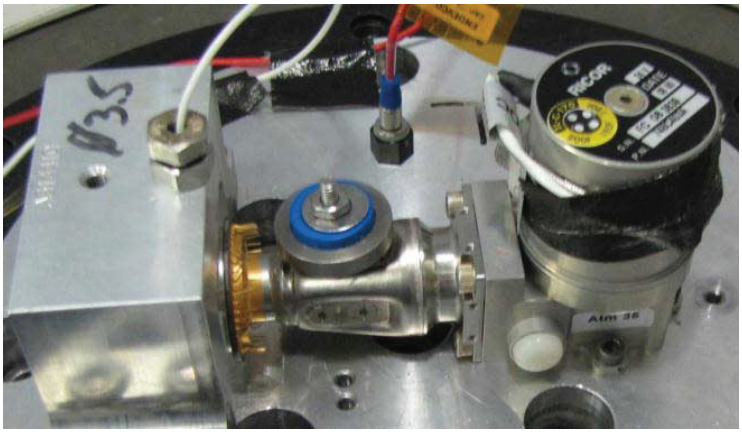

Figure 10. Experimental setup

The said IDDA is mounted upon the shaker table and is subjected to the above mentioned random vibration profile 5g rms with uniform PSD over the frequency range 10-2000Hz.

Figure 11 compares the experimentally evaluated absolute transmissibilities (a), PSDs of acceleration (b) and relative deflection (c) of the FPA before (bold solid curves) and after (dotted curves) mounting the wideband dynamic absorber.

In Figure 11, the double-lined curves present the theoretical predictions corresponding to the case of the optimal dynamic absorber. From Figure 11, application of a wideband dynamic absorber adding only 2% to the IDDA weight yields essentially a 3-fold attenuation of the FPA dynamic responses, in both acceleration and relative deflection. The theoretical predictions are in good agreement with experimental findings. In particular, the theoretical prediction indicated that the FPA dynamic responses (relative deflection and acceleration) may be attenuated to2.4µm rms and 26 g rms, while the experimental testing has shown attenuation to 2.7µm rms and 27 g rms, respectively. Any discrepancies may be partially explained by the inexact tuning of the properties of the dynamic absorber to their optimal values.

The ruggedized IDA described above has then been subjected to a half-sine shock 1000g@1 ms per MIL-STD 810F. Figure 12 compares the time histories of acceleration (a) and relative deflection (b) before (ref) and after mounting the wideband dynamic absorber. From Figure 12, the dynamic absorber drastically improves the settling time along with relieving the dynamic stresses during the entire transient process.

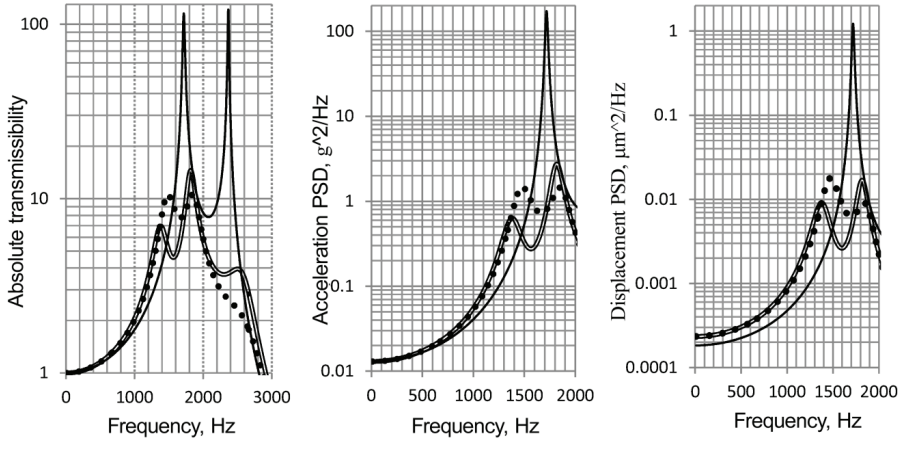

(a) (b) (c)

Figure 11. Comparison of experimental data and theoretical prediction

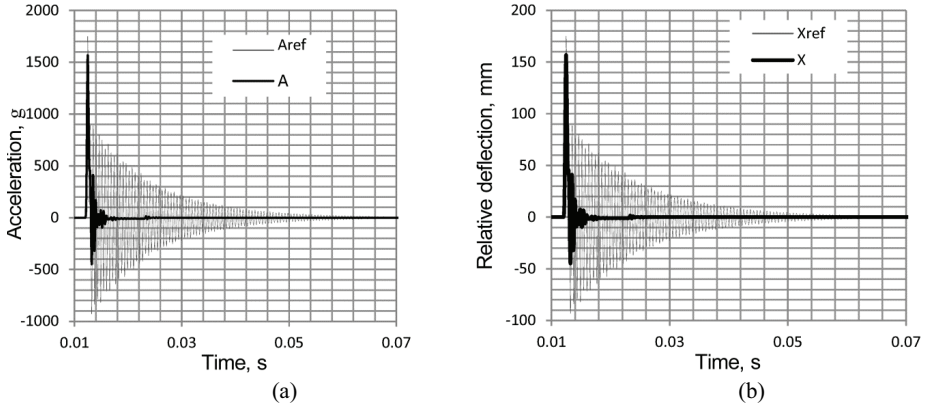

(a) (b)

Figure 12. Attenuation of dynamic response to a half-sine 1000g@1 ms shock.

CONCLUSIONS

The authors have shown the limitations of a state of the art technique for controlling the dynamic responses of the FPA by using a front support member. Upon observing the strong dynamic coupling between the FPA and the dewar envelope, they proposed the external mounting of a lightweight wideband dynamic absorber upon the dewar envelope structure. By adding only 2% to the IDDA weight they have achieved impressive attenuation of the FPA dynamic response both in terms of relative deflection and absolute acceleration, under typical random vibration and shock tests.

A theoretical model has been presented, based on the actual set of measured frequency response functions, and the theoretical predictions are in close agreement with the experimental findings. The authors have proposed how an optimal design may be obtained and have provided a sensitivity analysis.

Future work will include the design modifications of the evacuated dewar envelope and wideband dynamic absorber, and testing of attainable performance and qualification testing.

REFERENCES

1. Filis, A., Pundak, N., Zur, Y., Broyde, R. and Barak, M., "Cryocoolers for infrared missile warning systems," *Proc. SPIE*, Vol. 7660 (2010), pp. 76602L.

2. Ben Nun, U., Sanchez, J. P. and Lei, X., "Ruggedized integrated detector cooler assembly," US Patent 2012/0079838 A1 (2012).

3. Gallagher, B.W., Blionas, C., Nicolosi, J. A. and Barbara, R., "Closed cycle gas cryogenically cooled radiation detector," US Patent US5811816 A (1998).

4. Li Ran, et al, “Annular supporting structure of inner tube thin-wall portion of micro metal dewar”, China Patent CN 203203713 U (2013).

5. Nesher, O., Pivnik, I., Ilan, E., Calalhorra, Z., Koifman, A., Vaserman, I., Schlesinger, J.O., Gazit, R., Hirsh, I., "High resolution 1280x1024, 15 μm pitch compact InSb IR detector with on-chip ADC," *Proc. SPIE*, Vol. 7298 (2009), pp. 72983K.

6. Veprik, A., Babitsky, V., Pundak, N., Riabzev, S., "Suppression of cryocooler-induced microphonics in infrared imagers", *Cryogenics*, Vol. 49 Issue :8 (2009), pp. 449–454.

7. Ho, V., Veprik, A., Babitsky, V., "Ruggedizing printed circuit boards using a wideband dynamic absorber", *Shock and Vibration*, Vol. 10(3) (2001), pp. 195-210.